ACS central science

http://pubs.acs.org/journal/acscii

Research Article

Dehydration Enhances Prebiotic Lipid Remodeling and Vesicle Formation in Acidic Environments

Luke H. Steller, Martin J. Van Kranendonk, and Anna Wang*

Cite This: *ACS Cent. Sci.* 2022, 8, 132–139

Read Online

ACCESS | Metrics & More | Article Recommendations | Supporting Information

ABSTRACT: The encapsulation of genetic polymers inside lipid bilayer compartments (vesicles) is a vital step in the emergence of cell-based life. However, even though acidic conditions promote many reactions required for generating prebiotic building blocks, prebiotically relevant lipids tend to form denser aggregates at acidic pHs rather than prebiotically useful vesicles that exhibit sufficient solute encapsulation. Here, we describe how dehydration/rehydration (DR) events, a prebiotically relevant physicochemical process known to promote polymerization reactions, can remodel dense lipid aggregates into thin-walled vesicles capable of RNA encapsulation even at acidic pHs. Furthermore, DR events appear to favor the encapsulation of RNA within thin-walled vesicles over more lipid-rich vesicles, thus conferring such vesicles a selective advantage.

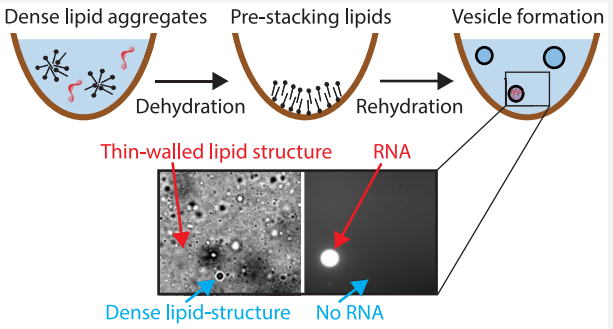

INTRODUCTION

Protocells, the hypothetical precursor to the first biological cell, likely consisted of a self-replicating genome encapsulated within a membrane vesicle.[1] The membrane would have played key roles in protocell function, such as promoting prebiotic reactions,[2] protecting protocells from parasitic genetic material,[3] and defining an individual replicating unit that could potentially become capable of growth and division, Darwinian competition, and subsequent evolution.[4,5]

One commonly proposed class of lipid molecules that could have formed prebiotic membranes are fatty acids.[6] Fatty acids were abiotically available, produced from both exogenous sources such as meteorites[7] and endogenous sources such as Fischer−Tropsch-like synthesis on Earth.[8] Importantly, fatty acids spontaneously form vesicles when the pH of the solution is near the apparent pK_a of the fatty acid, for example, between approximately pH 7 and 9 for decanoic acid.[6] The pH range for stability is determined by the fraction of carboxylic acid groups that are deprotonated, with complete protonation leading to the formation of a neat oil phase and complete deprotonation leading to micelle formation.[9] Of all of the self-assembled structures possible, oligolamellar or thin-walled vesicles are the most effective structures for encapsulation because they have a semipermeable membrane that delineates an internal aqueous volume. In contrast to dense lipid droplets or very multilamellar (or thick-walled) vesicles, they also most closely resemble the cells of modern organisms.

The narrow pH range of vesicle stability constrains the environments in which fatty acid vesicles can form. Multiple studies have raised the conundrum that because fatty acid vesicles could not have formed in acidic conditions, then neither could life.[10,11] Many important prebiotic reactions, including RNA polymerization[12] and nucleotide activation chemistry,[13] are optimized in acidic conditions. The Archean oceans are proposed to be acidic.[14] While mixtures of fatty acids with their corresponding alcohol or monoglyceride are capable of withstanding more alkaline conditions or higher salt concentrations,[15] fatty acid mixtures are generally observed to form dense oil droplets in acidic solutions,[16,17] unless prebiotically implausible cationic lipids such as sodium dodecylbenzenesulfonate,[18] or more complex lipids such as cyclophospholipids or *N*-acyl amino acids, are used.[10,19] Recently, Bonfio et al.[13] reported the formation of a small fraction of decanoic acid:decanol:decanal (4:1:1) vesicles alongside oil droplets and aggregates in the presence of 100 mM 4,5-dicyanoimidazole (DCI) buffer at pH 5.5. What is still unknown is whether a vesicle phase can be strongly favored at low pHs, or indeed whether vesicle formation is even possible in the absence of high DCI concentrations.

In one previous study, Milshteyn and co-workers observed a 12-carbon fatty acid/monoglyceride system form vesicles in unfiltered hot spring fluids at pH 3.3.[20] While it is a proof of concept, a major cause of hot spring pool acidity is dissolved gases (e.g., SO_2 and CO_2), and thus, fluid samples taken in the

Received: November 7, 2021
Published: January 7, 2022

field can degas after collection.[21,22] Because vesicle imaging in the previous study occurred up to six months from the time of sampling and vesicle samples were heated during imaging, it is highly likely that the pH of the vesicle solution when imaged had increased from the time of measurement in the field. Furthermore, the critical effects of dissolved salts[23] and organic materials[24,25] were not controlled for, with the authors stating that "an explanation is still uncertain".

In this current study, we take a more controlled approach by monitoring the sample pH and using nonvolatile acids, while using a significantly more selective RNA dye and controlling for dissolved matter, to better understand the system. We exploit the dynamic nature of fatty acid lipid assemblies and use dehydration/rehydration (DR) events to remodel dense lipid assemblies into vesicles possessing a large aqueous lumen. DR events are significant in prebiotic research because they would have been commonplace on exposed land surfaces on early Earth, ranging from micro-events induced by humidity[26] to larger events in daily tidal pools and even yearly weather patterns.[27] Hot springs are of particular interest as an environment capable of protocell production, as they not only display regular DR events on a range of time scales but also can capture meteor-delivered organics, concentrate prebiotically essential elements, and were likely present on the early Earth's surface when life was forming.[28,29]

While DR events are known to enable encapsulation of solutes such as genetic material into bilayer vesicles,[6,30,31] the ability of DR to favor certain vesicle topologies, or remodel membranes, has not been previously investigated. Recently, Sankar et al. explored how multiple DR events (referred therein as wet/dry cycles) affected bulk vesicle properties such as turbidity and dye encapsulation, demonstrating that lipid systems can undergo multiple DR events and still maintain their ability to form vesicles and encapsulate solutes.[32]

In this work, we focus on understanding the effect of a single DR event on remodeling prebiotically plausible lipid mixtures at the individual vesicle level, leading to encapsulation of RNA. In particular, we use microscopy to glean insight into population heterogeneity rather than average properties of a bulk sample. By doing so, we demonstrate that a single DR event can remodel dense lipid aggregates into vesicles at acidic pH. Furthermore, by using a fluorescent dye that targets single-stranded RNA with excellent selectivity, we show that DR biases the encapsulation of RNA and other solutes into vesicles that have thinner walls (oligolamellar), rather than thicker walls (very multilamellar). Vesicles containing more encapsulated solute have been shown to grow at the expense of vesicles with lower solute loading.[4] Our work thus demonstrates that DR events have the potential to not only remodel lipids into protocells at lower pHs but also provide a selective advantage to vesicles that have an architecture more akin to modern cell membranes.

RESULTS

Thin-Walled Vesicles Encapsulate RNA whereas Multilamellar Vesicles Do Not. We initially examined vesicle formation of the well-accepted prebiotic mixture of decanoic acid and glycerol monodecanoate (DA and GMD) at a pH near the apparent pK_a of decanoic acid. In a system buffered with PBS (phosphate-buffered saline) at pH 7.4, vesicles spontaneously formed after slight agitation of lipid (30 mM DA:GMD, 1:1), as observed by bright-field (no phase ring) microscopy (Figure 1A). We chose this pH to optimize

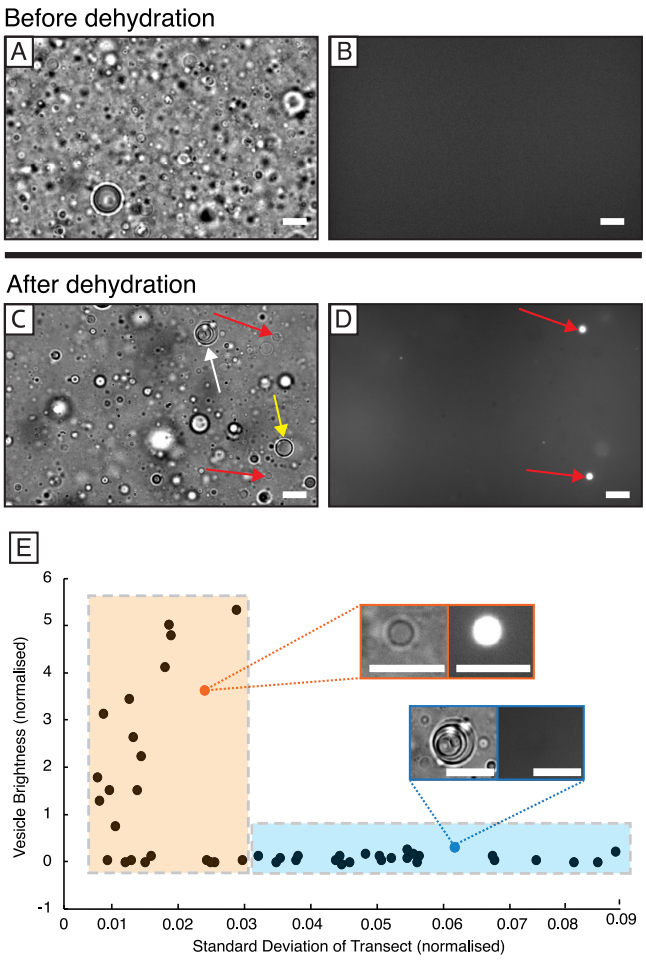

Figure 1. DA:GMD vesicles with RNA and QuantiFluor (RNA dye) in 1× PBS buffer (pH 7.4): (A) System before dehydration. Bright-field microscopy confirms that vesicles are present. (B) Fluorescence microscopy shows that no biased encapsulation of the RNA has occurred. (C) After one DR event, vesicles are still present, including thin-walled vesicles (orange arrows), multilamellar vesicles (white arrow), and thicker-walled vesicles (yellow arrow). (D) Fluorescence microscopy reveals that enhanced RNA encapsulation (orange arrows) occurs only within thin-walled vesicles. (E) After a single DR event, enhanced encapsulation occurred for some thin-walled vesicles. This graph depicts the normalized vesicle brightness, a proxy for amount of material encapsulated, against the standard deviation of a vesicle transect in bright-field, a proxy for vesicle wall lipid density for $N = 49$ vesicles (see the Experimental Section and Figure S2). The orange box outlines thin-walled vesicles (normalized transect value <0.03), and the blue box outlines multilamellar walled vesicles (normalized transect value >0.03). Scale bar represents 10 μm.

vesicle formation by working near the apparent pK_a of the lipid mixture (approximately 7.5[16]). As expected, when yeast RNA (0.1 mg/mL) along with a fluorescent RNA dye QuantiFluor was included in the buffer, no biased encapsulation was observed, as indicated by uniform fluorescence across the entire image (Figure 1B). This is because, without exposing the system to an encapsulation process, the RNA is evenly distributed throughout the sample.

We then subjected the DA:GMD and RNA aqueous system to a single DR event by evaporating to dryness via a heat bath (90 °C) and then rehydrating with Milli-Q water to mimic a natural dehydration event by heating, followed by rehydration from rainfall or a hot spring geyser.

https://doi.org/10.1021/acscentsci.1c01365
ACS Cent. Sci. 2022, 8, 132−139

Upon rehydration, a range of different vesicle morphologies formed, including oligolamellar thin-walled vesicles, multilamellar thick-walled vesicles, and multilamellar onion-like vesicles. However, while most vesicles exhibited minimal RNA encapsulation relative to the background, we observed that certain vesicle morphologies contained much higher concentrations of RNA (Figure 1C,D).

To understand this uneven encapsulation better, we use two imaging modalities to investigate the observed bias in encapsulation. The broader encapsulation process has been reported in previous works, with Deamer and Barchfeld first proposing solute entrapment between lipid membranes during dehydration and then subsequent vesicles budding off during rehydration as a method of encapsulation.[30] However, in some previous studies, cationic dyes were used to visualize the RNA and thus also labeled the anionic fatty-acid-based membranes.[20] To confirm this, we tested a commonly-used RNA dye (acridine orange) at the amounts used in these previous studies and found that it readily labeled fatty acid vesicles even in the absence of RNA (Figure S1). As a result, the localization of RNA as opposed to lipid should only be inferred indirectly when acridine orange and other cationic dyes are used.

Instead, we use a recently developed RNA dye that selectively labels single-stranded RNA to better probe the system. Additionally, we exploit the fact that the variation in bright-field microscopy intensity corresponds to optical density (and by proxy, material density) to quantitatively distinguish between vesicle types in a label-free manner. Oligolamellar and multilamellar vesicles can be distinguished by measuring the intensity of light in a transect across the vesicle in bright-field microscopy and taking the standard deviation of intensity across the transect (Figure S2).

We find that when vesicle brightness under fluorescence microscopy (a proxy for RNA encapsulation) is plotted against the standard deviation of vesicle intensity transects (a proxy for wall thickness) for each vesicle, there is a clear correlation between low membrane optical density (i.e., thin-walled vesicles) and increased RNA encapsulation (Figure 1E). In other words, while not all oligolamellar vesicles necessarily have high solute loading, the optical micrographs show that there is a clear trend of enhanced RNA encapsulation occurring almost exclusively within oligolamellar thin-walled vesicles (as opposed to thick-walled multilamellar vesicles) (Figure 1C,D). While previous studies have observed that DR events can lead to the formation of vesicles that exclude RNA,[20,30] our results show that some vesicles may in fact have the opposite behavior.

We also repeat our single DR event experiment with a well-known membrane label (Rhodamine B) and encapsulation marker (pyranine) instead of RNA. Again, we observe that the vesicles encapsulating the fluorescent pyranine dye are thin-walled (Figure 2A–D), as confirmed by taking transects across the fluorescence images (Figure 2E,F). Pyranine is clearly encapsulated within a lipid envelope (Figure 2E), whereas lipid-dense vesicles encapsulate very little pyranine (Figure 2F). These fluorescence microscopy results confirm that when biased encapsulation does occur, the vesicles with enhanced solute encapsulation are thin-walled vesicles rather than thick-walled (see also Figure S3). In other words, thin-walled vesicles are conferred an advantage by DR events.

To determine if selective encapsulation within thin-walled vesicles was exclusive to decanoic acid systems, we use a different lipid system, oleic acid (OA) and glycerol monooleate

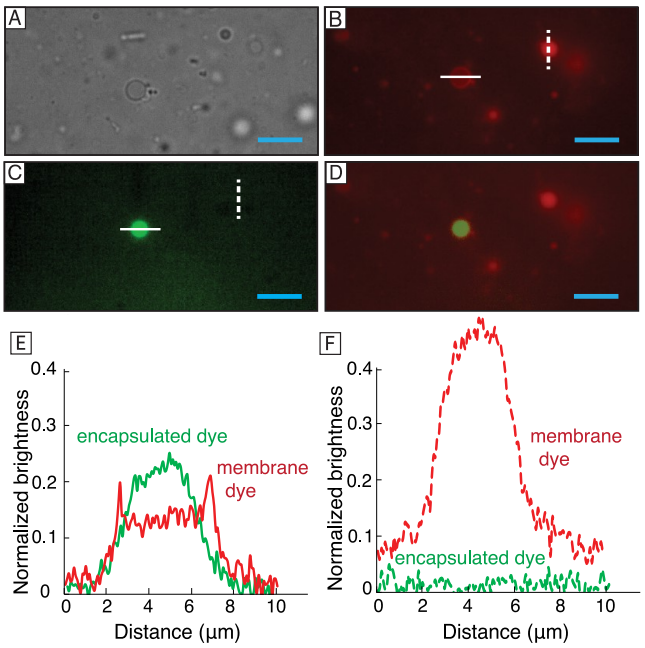

Figure 2. DA:GMD vesicles with pyranine as the encapsulation molecule (no RNA) in 1× PBS buffer (pH 7.4) after a single dehydration event: (A) Bright-field microscopy image of sample. (B) The Rhodamine B fluorescence channel shows that a mixture of vesicle types are present in the system after rehydration, including thin-walled (white solid line) and thick-walled (white dotted line) vesicles. (C) Pyranine fluorescence channel. (D) Composite image of Rhodamine B and pyranine channels. (E) Gray-value transect of Rhodamine B (red) and encapsulated pyranine (green) demonstrating encapsulation within the thin-walled vesicle, compared to a (F) transect of a thick-walled multilamellar vesicle (white dotted line in panels B and C). See the Experimental Section for further details of image analysis. Scale bars in blue represent 12 μm. Additional examples of Rhodamine B/bright-field/pyranine vesicle image sets demonstrating vesicle formation and encapsulation can be found in Figure S3.

(GMO). Because the melting point of GMO is approximately 40 °C, we use a 2:1 OA:GMO ratio rather than 1:1 to avoid working with a gel-phase bilayer. After a DR event in PBS buffer (adjusted to pH 8.2 using NaOH), we find similar results to the DA:GMD system, i.e., that the vesicles that exhibit biased encapsulation are also thin-walled (Figure S4).

Dehydration/Rehydration Events Remodel Dense Lipid Aggregates into Vesicles at a pH below Their pK_a. The effects of a DR event on lipid vesicles are more profound at acidic pHs. When 30 mM of total lipid (1:1 DA:GMD) is added to an unbuffered solution of 10 mM NaCl and 0.1 mg/mL yeast RNA, the resulting pH is 5.4. Whereas an abundance of vesicles was observed under bright-field in the pH 7.4 system buffered with PBS, at pH 5.4, the lipid mixture forms optically dense spheres that have a propensity to wet the glass slides, indicative of their high surface energy. Under fluorescence microscopy, no biased encapsulation is observed (Figure 3A,B). These results are consistent with previous results, where a decanoic acid decanol mixture was not able to form vesicles at pH 5.5,[6,33] and a decanoic acid/decanal/decanol mixture was only observed to have a small fraction of vesicles present at pH 5.5.[13]

However, when we expose our lipid system to a single DR event, the optically dense spheres remodel to form a diverse range of vesicles, similar to those observed in the pH 7.4

https://doi.org/10.1021/acscentsci.1c01365
ACS Cent. Sci. 2022, 8, 132−139

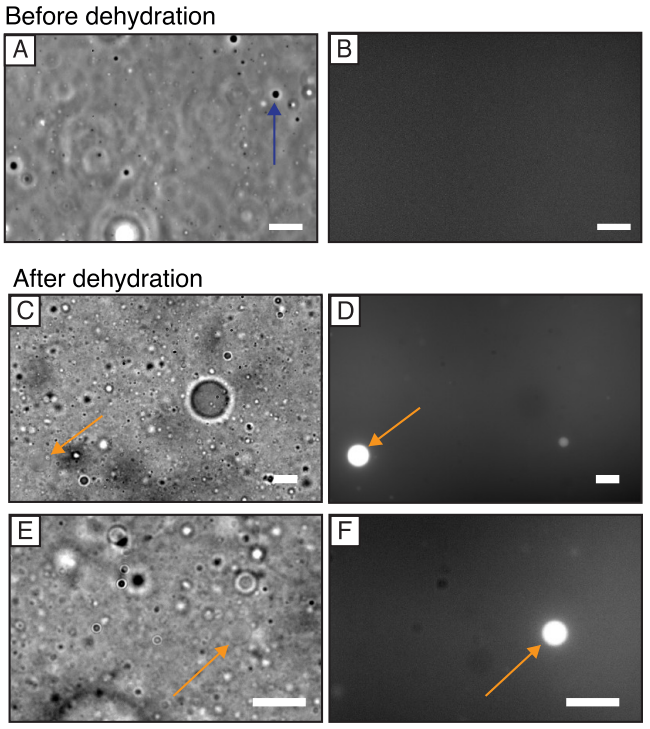

Figure 3. DA:GMD vesicles with RNA and QuantiFluor (RNA dye) in 10 mM NaCl solution (pH 5.4). (A) Before dehydration, the lipid forms dense aggregates because the solution is below the apparent pK_a of the fatty acid (blue arrow). (B) The solution exhibits homogeneous fluorescence indicating that RNA is evenly dispersed through the solution. (C−F) One DR event remodels the lipid to form a wide range of vesicles, including thin-walled vesicles that show enhanced RNA encapsulation (orange arrows). Panels A, C, and E are bright-field optical micrographs; panels B, D, and F are fluorescence images. Scale bar represents 10 μm.

system. These remodeled vesicles are capable of encapsulating RNA in solution, again with enhanced encapsulation in some thin-walled vesicles (Figure 3C−F). No observable change is measured in the pH of the solution after rehydration. This effect is confirmed in a buffered acidic system: When DA:GMD is mixed into 0.01 M citrate buffer (pH 5.3), it only forms dense lipid droplets that wet surfaces. After one DR event, however, it forms a large range of vesicle morphologies (Figure S5). We find that the lipid system buffered at pH 3.9 with 0.01 M citrate does not form vesicles upon rehydration, indicating a lower pH limit for the remodeling phenomenon (Figure S5).

We also confirm that although the remodeled vesicles are capable of encapsulating RNA present within solution, lipid remodeling is not driven by the specific chemical or ionic nature of the encapsulated molecules. This phenomenon is reproduced using an uncharged encapsulation material (sucrose) as well as with no additional encapsulation material present. In both instances, dense lipid aggregates remodel into thin-walled vesicles after rehydration (Figures S6 and S7).

Finally, we verify that dehydration/rehydration is not dramatically shifting the equilibrium of self-assembled structures. We use the lipid probe Laurdan to reveal the polarity of the probe's environment: a single emission peak at 450 nm indicates a droplet phase for fatty acids, whereas peaks at 430 and 500 nm indicate the presence of lipid bilayer vesicles.[32] We confirm that the optically dense spheres that we see at pH 5.5 are in fact a bilayer phase (Figure S8). An increase in Laurdan generalized polarization (GP, see the Experimental Section and Figure S8) values is also consistent with DR appearing to remodel the lipids from being in a very dense, multilamellar form, into vesicles that have larger interlamellar spacing.

DISCUSSION

Our research presents evidence for a purely physical remodeling method to form fatty acid vesicles, enabling increased encapsulation inside oligolamellar vesicles even at acidic pHs. Because heating was used to accelerate dehydration in our experiments, we questioned whether heat itself was driving the remodeling, as previous work has noted that elevated temperatures can cause temporary phase transitions (i.e., melting) for both phospholipids[34] and fatty acids[35,36] that lead to vesicle formation at higher temperatures. However, this is a transient effect, as vesicles formed in these systems transform back into dense lipid droplets or crystals once the temperature is reverted back to room temperature. Despite DA and GMD being solids at room temperature, a 1:1 combination of the two results in a mixture that is a liquid at room temperature (Figure S9). This eliminates lipid heating as a primary driver for vesicle remodeling in this system, because the fatty acid mixture is already a liquid at room temperature. This was confirmed experimentally: when pH 5.4 DA:GMD solution was dried down with passive evaporation at room temperature (~20 °C), the lipid still remodeled to form vesicles similar to those formed after drying at elevated temperatures (Figure S10). Regardless of drying temperature, the vesicles produced by our method are stable at room temperature, demonstrated by all vesicles microscopy images being captured at ~20 °C. In fact, this vesicle system is stable for long time periods after initial remodeling, still containing thin-walled vesicles nearly 11 months after they first formed (Figure S11). We can therefore rule out heat itself as a driver for lipid remodeling.

While heat is not a major factor in these experiments, the dispersal of lipid within an aqueous solution is crucial for lipid remodeling to occur. Lipids are commonly dissolved non-aqueous solvents as a first step toward creating vesicles.[37,38] However, when a DA:GMD mixture was added to methanol instead of water or aqueous buffer and then dried down, only emulsion droplets were observed upon rehydration (Figure S12). Methanol is an excellent solvent for the lipids and therefore does not promote any lipid self-assembly. Removal of methanol by dehydration simply leads to amorphous oil droplets forming. By contrast, attempts at dispersing the lipids into aqueous solution result in lipids preorganizing via hydrogen bonding and hydrophobic forces.

One additional factor is that sufficient amphiphilicity is required to ensure lipid remodeling. At pH 3.9, too few DA are ionized to support bilayer formation (Figure S5). We also tried the experiment at pH 5.5 with other lipids with smaller headgroups than GMD. When this experiment was repeated with pure decanoic acid (DA), without GMD present, the DA formed a neat oil droplet at the bottom of the microcentrifuge tube after dehydration at 90 °C. Upon rehydration, the bulk solution was clear with solidified decanoic acid adhering to the side of the microcentrifuge tube, and no oligolamellar vesicles were present under phase contrast microscopy (Figure S13). No vesicles were observed when the experiment was also repeated with a 4:1 mixture of decanoic acid and decanol

https://doi.org/10.1021/acscentsci.1c01365
ACS Cent. Sci. 2022, 8, 132−139

(Figure S13). We hypothesize that this is because, at pH 5.5, DA alone and the DA:DO mixture remain an interfacially inactive oil. In other words, without ionizing the DA, the polarity of the headgroups is simply too low to support bilayer formation. The addition of GMD with its substantial headgroup is crucial in this process, as it also is to protocell thermostability.[39]

Proposed Model for Membrane Remodeling. We imaged the lipid before and after a dehydration event to determine what type of restructuring takes place. Before dehydration, the DA:GMD mixture is an oil that spreads as a droplet on the microscope slide (Figure S14). Upon mixing with a simple 10 mM NaCl solution and subsequent dehydration without rehydration, complex heterogeneous structures formed. These include layered lipid structures showing birefringence under crossed polarizers and halite crystals incorporated into lipid aggregates (Figure S14). This suggests that physical restructuring and prestacking of lipid is contributing to lipid remodeling upon rehydration. We propose two separate effects that are promoting lipid remodeling: physical prestacking of lipid membranes owing to evaporation, and osmotically-driven swelling of lipids during rehydration (Figure 4).

During dehydration, solutions are concentrated, and thus, the ionic strength increases with time. Interestingly, the apparent pK_a of fatty-acid-based vesicles depends on ionic strength. Maeda et al.[40] reported salt dependence in the titration curve of oleic acid, with the apparent pK_a decreasing by 0.7 upon an increase in ionic strength from 10 mM NaCl to 100 mM NaCl. Mele et al.[41] modeled that the apparent pK_a for oleic acid decreases by 2.2 upon an increase in ionic strength from 1 to 150 mM NaCl. This behavior is predicted by the Poisson−Boltzmann equation. In brief, charged surfaces such as fatty acid bilayer membranes recruit counterions, including protons, reducing the pH of the surface. The apparent pH at the bilayer surface is thus lower than the bulk pH, leading to an increase in the apparent pK_a of the fatty acid. An increase in salt concentration decreases the efficiency of proton recruitment to the interface, leading to a smaller apparent pK_a shift. Thus, as the solution evaporates, we expect the apparent pK_a of the lipid to decrease to lower pHs. If the pH of the sample decreases minimally or stays constant owing to buffering agents, the deprotonation of the membrane is expected to increase with evaporation, thereby favoring lipid deprotonation (Figure 4A). The negatively charged carboxylate residues can then interact more strongly with cations such as sodium ions, hereby forming preorganized lipid layers upon further dehydration (as shown in Figure S14). This physical stacking of lipid during dehydration plays a crucial role in this system, as simply increasing the salt concentration of a DA:GMD lipid system at pH 5.5 without any dehydration event does not result in vesicle formation (Figure S15). Increasing the ionic strength for an oleic acid solution at pH 8.06, however, does promote oligolamellar vesicle formation in lieu of dense aggregates (Figure S16), highlighting the complex impact of salt. Upon rehydration with water, well-separated bilayer structures may be able to form more readily from these preorganized sheets than from homogeneous oil droplets, leading to an increase in vesicles as opposed to dense lipid-rich aggregates.

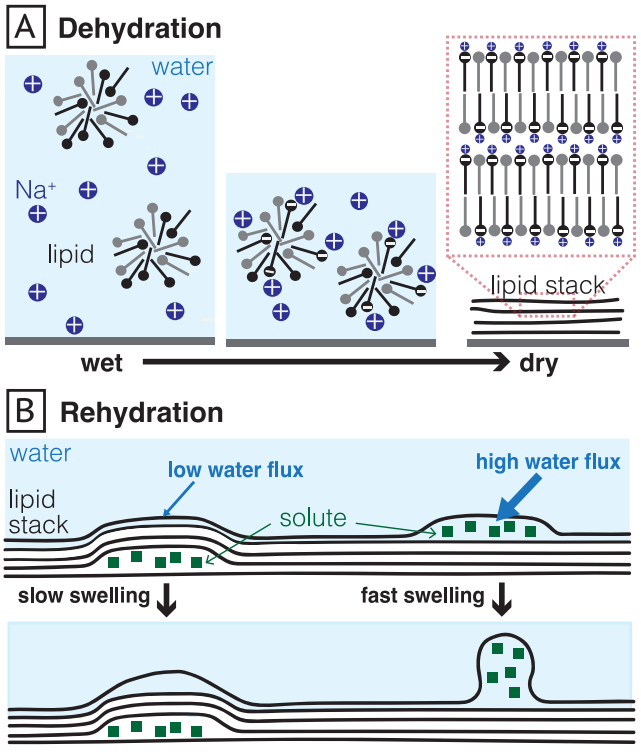

Figure 4. (A) During dehydration, solutes such as sodium ions (blue) as well as aggregates of nonionizable lipid (glycerol monodecanoate, gray) and ionizable lipid (decanoic acid, black) are concentrated. An increase in ionic strength leads to a decrease in decanoic pK_a, deprotonating the decanoic acid. These ionized groups can then interact with sodium cations and form preorganized lipid layers. (B) Rehydration preferentially swells pockets of solute molecules (green) that are bound by fewer bilayers.

Encapsulation within Oligolamellar Vesicles. There is an additional process occurring in the DA:GMD system (at both pH ranges) that is promoting encapsulation of solutes (including RNA) within oligolamellar vesicles over multilamellar vesicles. During rehydration, there is a large osmotic driving force for preorganized lipids that are colocalized with solute to be hydrated. The rate of lipid swelling and vesicle formation is then determined by water permeation across the membrane. The flux of water J across the lipid is related to the solute concentration difference across the membrane Δc by $J = P\Delta c/n$ where P is the permeability of water across a single bilayer, and n is the number of bilayers across which water needs to permeate. When solute is trapped underneath a thick layer of lipid, water permeates slowly, and the lipid film swells at a slower rate. Conversely, when pockets of solute are trapped underneath a thin layer of lipid, water is able to readily permeate across the lipid layers and swell the film, leading to the formation of solute-rich oligolamellar vesicles (Figure 4B).

More broadly, it appears that an increase in interlamellar spacing is an observed consequence of both a dehydration/rehydration cycle for fatty acid/monoglyceride admixtures, as well as during freeze/thaw cycles for phospholipids.[42] Commonalities between the two processes include the dehydration of the lipid bilayer potentially leading to membrane fusion, and osmotic imbalances potentially leading to inhomogeneous swelling of bilayers. Both processes could have occurred in surficial systems and worked in alternate seasons to promote protocell formation and solute encapsulation.

Origin of Life Implications. This research provides new insight into the environmental conditions suitable for forming

https://doi.org/10.1021/acscentsci.1c01365
ACS Cent. Sci. 2022, 8, 132−139

life on Earth. Our findings open up new regions of geochemical parameter space, creating the potential for prebiotically plausible vesicles to form in acidic conditions, making encapsulation accessible to chemical reactions that favor lower-pH environments (e.g., RNA polymerization).[2]

Furthermore, DR appears to confer an advantage to thin-walled protocells owing to their increased encapsulation of prebiotically useful macromolecules relative to other vesicle types. These oligolamellar vesicles are closer in morphology to the unilamellar membranes that encapsulate modern cells[43] and may also be more prebiotically preferable because of their increased permeability.[44] This is because membrane permeability is an important feature in biology, with cells possessing pumps and pores to allow the exchange of material. Multilamellar thick-walled vesicles would have been a disadvantage for early protocells, restricting the exchange of food and waste with the surrounding environment.[1] A protocell formation process that biases encapsulation of solutes into thin-walled vesicles, which are relatively permeable and readily exchange material with their environment, could have been extremely advantageous. Although this study focused on the effects of a single DR event, it has been clearly shown in other studies that fatty acid vesicle systems can undergo multiple DR events and still maintain their ability to form vesicles and encapsulate solutes,[32] increasing its suitability as a potential prebiotic protocell system.

Our findings provide new insight into the ongoing debate on whether surficial pools[45] or deep-sea hydrothermal vents[46] were the environment in which life formed on Earth. As the observed fatty acid vesicle stability in acidic conditions and selective encapsulation within thin-walled, cell-like vesicles relies on dehydration as a physical remodeling process, this research serves as further evidence against life forming in permanently submerged vents because they are incapable of widespread dehydration events.

Lastly, our findings highlight that special attention should be given to the method of vesicle formation and hence the path of lipid assembly when comparing results from different studies. This is because while prebiotically plausible lipids are vastly more soluble and their assemblies more dynamic than their phospholipid counterparts, prebiotic lipid systems are still capable of being kinetically trapped and are not true equilibrium systems.[47] In the origins of life field, researchers use a range of vesicle preparation methods such as titration,[48] thin film hydration,[10] wet/dry cycling with varying surfaces and solvents,[20,49] self-assembly with and without shear,[43] (for example and extrusion. These different methods can have a substantial effect on the resulting vesicle characteristics, as they are well-known to do for phospholipids.[50] While this provides exciting opportunities to the variety of different membrane-bound architectures that may have been present on early Earth, it also necessitates care when comparing vesicles produced by different methods.

EXPERIMENTAL SECTION

Reagents. For RNA solution (10 mg/mL, ribonucleic acid from torula yeast, Type VI, Sigma-Aldrich), 100 mg of yeast RNA was added to 10 mL of 10 mM EDTA solution (ChemSupply Australia) in Milli-Q water. The RNA solution was adjusted to pH 6 with 5 M NaOH (Lowy Solutions). The QuantiFluor RNA System (Promega) was used as the RNA dye; other dyes used include 1 mM pyranine (Sigma-Aldrich) as an encapsulation marker, 0.1 mM acridine orange as a commonly-used cationic dye, and 5 μm Rhodamine B (Sigma-Aldrich) as a membrane dye. Sucrose (ChemSupply Australia) at 0.1 M was also used as a neutral encapsulation molecule. Buffers used include 1× PBS made from 10× PBS stock solution (Lowy Solutions) and 0.01 M citrate buffer (ChemSupply Australia), with pH adjusted with 5 M NaOH or HCl (Lowy Solutions). NaCl solutions (10 mM) were made by appropriate dilutions of 5 M NaCl solution (Lowy Solutions). pH was measured using an Orion Star A121 pH meter with an Orion 8103BN ROSS probe.

Vesicle Preparation. All reagents for each specific experiment, including the appropriate lipid, encapsulation solutes, and buffers, were added to the Eppendorf tube, vortexed for 15 s, and then agitated by scraping the tube three times against a microcentrifuge rack ("rumble-stripped"[51]). Tubes selected for dehydration were then partly submerged in a heat bath (90 °C) for 1 h. For analysis, dehydrated samples were rehydrated with 100 μL of Milli-Q water directly before analysis. Both samples (dehydrated and non-dehydrated) were rumble-stripped 5 times before microscope analysis to distribute vesicles through sample fluid and ensure a representative selection of vesicles. Experiments were repeated a further three times on separate days with fresh stock solutions, with consistent results recorded each time.

Imaging. Images were captured on a pco.edge 4.2 sCMOS camera mounted on a Nikon Eclipse TE-2000 inverted microscope, using a 100× Ph3 objective [Plan Fluor, numerical aperture (NA) = 1.3]. We focused on the solution phase of the sample instead of focusing on the surface of the glass slide to ensure that imaging was representative of the whole solution and to avoid imaging vesicles that are known to grow from the surfaces of glass slides.[52]

Image Analysis. For Figure 1E, all vesicles larger than 5 μm visible in bright-field were analyzed, with a total of $N = 49$ across 12 bright-field micrographs and their 12 corresponding fluorescence micrographs.

Normalized Vesicle Brightness for Fluorescence Images. The intensity of encapsulated dye relative to the background was measured in Fiji.[53] The mean gray scale value for approximately 5 × 5 μm rectangles inside (I_{in}) and outside (I_{bg}) the vesicles was determined using the *measure* tool. The normalized vesicle brightness was calculated by $(I_{in} - I_{bg})/I_{bg}$.

Normalized Transect Standard Deviation for Bright-Field Images. Transects across vesicles T, including a background overlap on each side of the vesicle that is at least 10% of the total vesicle width on each side, were taken using the *line* tool and *plot profile* tool in Fiji.[53] The average of the first 10 pixels at the beginning of the transect was taken as the background value B. The transect T was then normalized against background T/B. The standard deviation σ of T/B was then reported as the normalized transect standard deviation.

Laurdan GP Measurements. 100 μL of a vesicle sample and 10 μM Laurdan (Sigma-Aldrich) were premixed in a microcentrifuge tube before being loaded into a quartz cuvette (Starna) and then into a Cary Eclipse fluorescence spectrometer (Agilent). Excitation was at 360 nm, and emission was measured from 400 to 600 nm. For fatty acids, the emission spectrum peaks are approximately at 430 and 500 nm,[32] so the generalized polarization GP is defined as $(I_{500} - I_{430})/(I_{500} + I_{430})$. By the definition used here, a highly polar environment such as micelles has GP ~ 1.[32]

Safety Statement. No unexpected or unusually high safety hazards were encountered.

https://doi.org/10.1021/acscentsci.1c01365
ACS Cent. Sci. 2022, 8, 132−139

■ ASSOCIATED CONTENT

Supporting Information

The Supporting Information is available free of charge at https://pubs.acs.org/doi/10.1021/acscentsci.1c01365.

Optical micrographs in phase contrast, bright-field, and epifluorescence mode; photographs of bulk samples; as well as details of analyses and fluorescence spectra (PDF)

■ AUTHOR INFORMATION

Corresponding Author

Anna Wang − *School of Chemistry and Australian Centre for Astrobiology, UNSW Sydney, Bedegal Country, New South Wales 2052, Australia;* orcid.org/0000-0002-2148-1996; Email: anna.wang@unsw.edu.au

Authors

Luke H. Steller − *School of Biological, Earth and Environmental Sciences and Australian Centre for Astrobiology, UNSW Sydney, Bedegal Country, New South Wales 2052, Australia*

Martin J. Van Kranendonk − *School of Biological, Earth and Environmental Sciences and Australian Centre for Astrobiology, UNSW Sydney, Bedegal Country, New South Wales 2052, Australia*

Complete contact information is available at: https://pubs.acs.org/10.1021/acscentsci.1c01365

Notes

The authors declare no competing financial interest.

■ ACKNOWLEDGMENTS

L.H.S. and M.J.V.K. are supported by the Australia Research Council Discovery Project DP180103204 awarded to M.J.V.K. A.W. is the recipient of an Australian Research Council Discovery Early Career Award (DE210100291). The authors would like to acknowledge and pay their respects to the Bedegal people, who are the traditional custodians of the land on which this research took place. We also thank Dr. Albert Fahrenbach, Prof. David Deamer, Lauren Lowe, and Daniel Loo for helpful advice and discussions.

■ REFERENCES

(1) Dzieciol, A. J.; Mann, S. Designs for life: protocell models in the laboratory. *Chem. Soc. Rev.* **2012**, *41*, 79−85.

(2) Rajamani, S.; Vlassov, A.; Benner, S.; Coombs, A.; Olasagasti, F.; Deamer, D. Lipid-assisted Synthesis of RNA-like Polymers from Mononucleotides. *Origins of Life and Evolution of Biospheres* **2008**, *38*, 57−74.

(3) Szathmáry, E.; Demeter, L. Group selection of early replicators and the origin of life. *J. Theor. Biol.* **1987**, *128*, 463−486.

(4) Chen, I. A.; Roberts, R. W.; Szostak, J. W. The emergence of competition between model protocells. *Science* **2004**, *305*, 1474−1476.

(5) Szostak, J. W.; Bartel, D. P.; Luisi, P. L. Synthesizing life. *Nature* **2001**, *409*, 387−390.

(6) Apel, C. L.; Deamer, D. W.; Mautner, M. N. Self-assembled vesicles of monocarboxylic acids and alcohols: conditions for stability and for the encapsulation of biopolymers. *Biochimica et Biophysica Acta (BBA) - Biomembranes* **2002**, *1559*, 1−9.

(7) Lai, J. C.-Y.; Pearce, B. K.; Pudritz, R. E.; Lee, D. Meteoritic abundances of fatty acids and potential reaction pathways in planetesimals. *Icarus* **2019**, *319*, 685−700.

(8) Rushdi, A. I.; Simoneit, B. R. Lipid formation by aqueous Fischer−Tropsch-type synthesis over a temperature range of 100 to 400 C. *Origins of Life and Evolution of the Biosphere* **2001**, *31*, 103−118.

(9) Meierhenrich, U.; Filippi, J.-J.; Meinert, C.; Vierling, P.; Dworkin, J. On the Origin of Primitive Cells: From Nutrient Intake to Elongation of Encapsulated Nucleotides. *Angew. Chem., Int. Ed.* **2010**, *49*, 3738−3750.

(10) Joshi, M.; Samanta, A.; Tripathy, G.; Rajamani, S. Formation and Stability of Prebiotically Relevant Vesicular Systems in Terrestrial Geothermal Environments. *Life* **2017**, *7*, 51.

(11) Morigaki, K.; Walde, P. Fatty acid vesicles. *Curr. Opin. Colloid Interface Sci.* **2007**, *12*, 75−80.

(12) Bernhardt, H. S.; Tate, W. P. Primordial soup or vinaigrette: did the RNA world evolve at acidic pH? *Biology Direct* **2012**, *7*, 4.

(13) Bonfio, C.; Russell, D. A.; Green, N. J.; Mariani, A.; Sutherland, J. D. Activation chemistry drives the emergence of functionalised protocells. *Chemical Science* **2020**, *11*, 10688−10697.

(14) Pinti, D. L. *Lectures in astrobiology*; Springer, 2005; pp 83−112.

(15) Maurer, S.; Deamer, D.; Boncella, J.; Monnard, P.-A. Chemical Evolution of Amphiphiles: Glycerol Monoacyl Derivatives Stabilize Plausible Prebiotic Membranes. *Astrobiology* **2009**, *9*, 979−987.

(16) Monnard, P.-A.; Deamer, D. W. *Methods in Enzymology*; Elsevier, 2003; Vol. *372*, pp 133−151.

(17) Morigaki, K.; Walde, P.; Misran, M.; Robinson, B. H. Thermodynamic and kinetic stability. Properties of micelles and vesicles formed by the decanoic acid/decanoate system. *Colloids Surf., A* **2003**, *213*, 37−44.

(18) Namani, T.; Deamer, D. W. Stability of Model Membranes in Extreme Environments. *Origins of Life and Evolution of Biospheres* **2008**, *38*, 329−341.

(19) Toparlak, Ö. D.; Karki, M.; Egas Ortuno, V.; Krishnamurthy, R.; Mansy, S. S. Cyclophospholipids increase protocellular stability to metal ions. *Small* **2020**, *16*, 1903381.

(20) Milshteyn, D.; Damer, B.; Havig, J.; Deamer, D. Amphiphilic Compounds Assemble into Membranous Vesicles in Hydrothermal Hot Spring Water but Not in Seawater. *Life* **2018**, *8*, 11.

(21) Taulis, M.; Milke, M. Chemical variability of groundwater samples collected from a coal seam gas exploration well, Maramarua, New Zealand. *Water research* **2013**, *47*, 1021−1034.

(22) Tahvanainen, T.; Tuomaala, T. The reliability of mire water pH measurements—a standard sampling protocol and implications to ecological theory. *Wetlands* **2003**, *23*, 701−708.

(23) Maurer, S. E.; Nguyen, G. Prebiotic vesicle formation and the necessity of salts. *Origins of Life and Evolution of Biospheres* **2016**, *46*, 215−222.

(24) Black, R. A.; Blosser, M. C.; Stottrup, B. L.; Tavakley, R.; Deamer, D. W.; Keller, S. L. Nucleobases bind to and stabilize aggregates of a prebiotic amphiphile, providing a viable mechanism for the emergence of protocells. *Proc. Natl. Acad. Sci. U. S. A.* **2013**, *110*, 13272−13276.

(25) Cornell, C. E.; Black, R. A.; Xue, M.; Litz, H. E.; Ramsay, A.; Gordon, M.; Mileant, A.; Cohen, Z. R.; Williams, J. A.; Lee, K. K.; et al. Prebiotic amino acids bind to and stabilize prebiotic fatty acid membranes. *Proc. Natl. Acad. Sci. U. S. A.* **2019**, *116*, 17239−17244.

(26) Campbell, T. D.; Febrian, R.; McCarthy, J. T.; Kleinschmidt, H. E.; Forsythe, J. G.; Bracher, P. J. Prebiotic condensation through wet-dry cycling regulated by deliquescence. *Nat. Commun.* **2019**, *10*, 4508.

(27) Westall, F.; Hickman-Lewis, K.; Hinman, N.; Gautret, P.; Campbell, K.; Bréhéret, J.; Foucher, F.; Hubert, A.; Sorieul, S.; Dass, A.; et al. A Hydrothermal-Sedimentary Context for the Origin of Life. *Astrobiology* **2018**, *18*, 259−293.

(28) Steller, L. H.; Nakamura, E.; Ota, T.; Sakaguchi, C.; Sharma, M.; Van Kranendonk, M. J. Boron Isotopes in the Puga Geothermal System, India, and Their Implications for the Habitat of Early Life. *Astrobiology* **2019**, *19*, 1459−1473.

(29) Van Kranendonk, M. J.; Baumgartner, R.; Djokic, T.; Ota, T.; Steller, L.; Garbe, U.; Nakamura, E. Elements for the Origin of Life on

Land: A Deep-Time Perspective from the Pilbara Craton of Western Australia. *Astrobiology* **2021**, *21*, 39−59.
(30) Deamer, D. W.; Barchfeld, G. L. Encapsulation of macromolecules by lipid vesicles under simulated prebiotic conditions. *Journal of Molecular Evolution* **1982**, *18*, 203−206.
(31) Damer, B.; Deamer, D. Coupled Phases and Combinatorial Selection in Fluctuating Hydrothermal Pools: A Scenario to Guide Experimental Approaches to the Origin of Cellular Life. *Life* **2015**, *5*, 872−887.
(32) Sarkar, S.; Dagar, S.; Rajamani, S. Influence of Wet-dry Cycling on the Self-Assembly and Physicochemical Properties of Model Protocellular Membrane Systems. *ChemSystemsChem.* **2021**, *3*, e2100032.
(33) Namani, T.; Walde, P. From decanoate micelles to decanoic acid/dodecylbenzenesulfonate vesicles. *Langmuir* **2005**, *21*, 6210−6219.
(34) Melchior, D. L.; Steim, J. M. Thermotropic Transitions in Biomembranes. *Annu. Rev. Biophys. Bioeng.* **1976**, *5*, 205−238.
(35) Hargreaves, W. R.; Deamer, D. W. Liposomes from ionic, single-chain amphiphiles. *Biochemistry* **1978**, *17*, 3759−3768.
(36) Maurer, S. E.; Tølbøl Sørensen, K.; Iqbal, Z.; Nicholas, J.; Quirion, K.; Gioia, M.; Monnard, P.-A.; Hanczyc, M. M. Vesicle Self-Assembly of Monoalkyl Amphiphiles under the Effects of High Ionic Strength, Extreme pH, and High Temperature Environments. *Langmuir* **2018**, *34*, 15560−15568.
(37) Reeves, J. P.; Dowben, R. M. Formation and properties of thin-walled phospholipid vesicles. *Journal of Cellular Physiology* **1969**, *73*, 49−60.
(38) Zhang, H.Thin-Film Hydration Followed by Extrusion Method for Liposome Preparation. *Liposomes. Methods in Molecular Biology*; Humana Press: New York, NY, 2017, Vol. *1522*. DOI: 10.1007/978-1-4939-6591-5_2.
(39) Mansy, S. S.; Szostak, J. W. Thermostability of model protocell membranes. *Proc. Natl. Acad. Sci. U. S. A.* **2008**, *105*, 13351−13355.
(40) Maeda, H.; Eguchi, Y.; Suzuki, M. Hydrogen ion titration of oleic acid in aqueous media. *J. Phys. Chem.* **1992**, *96*, 10487−10491.
(41) Mele, S.; Söderman, O.; Ljusberg-Wahrén, H.; Thuresson, K.; Monduzzi, M.; Nylander, T. Phase behavior in the biologically important oleic acid/sodium oleate/water system. *Chem. Phys. Lipids* **2018**, *211*, 30−36.
(42) Mayer, L. D.; Hope, M. J.; Cullis, P. R.; Janoff, A. S. Solute distributions and trapping efficiencies observed in freeze-thawed multilamellar vesicles. *Biochimica et Biophysica Acta (BBA) - Biomembranes* **1985**, *817*, 193−196.
(43) Kindt, J. T.; Szostak, J. W.; Wang, A. Bulk Self-Assembly of Giant, Unilamellar Vesicles. *ACS Nano* **2020**, *14*, 14627−14634.
(44) Thomas, J. A.; Rana, F. The influence of environmental conditions, lipid composition, and phase behavior on the origin of cell membranes. *Origins of Life and Evolution of Biospheres* **2007**, *37*, 267−285.
(45) Damer, B.; Deamer, D. The hot spring hypothesis for an origin of life. *Astrobiology* **2020**, *20*, 429−452.
(46) Russell, M. J. The ater Problemsic), the Illusory Pond and Lifeas Submarine Emergence Review. *Life* **2021**, *11*, 429.
(47) Luisi, P. L. Are Micelles and Vesicles Chemical Equilibrium Systems? *J. Chem. Educ.* **2001**, *78*, 380.
(48) Jordan, S. F.; Rammu, H.; Zheludev, I. N.; Hartley, A. M.; Maréchal, A.; Lane, N. Promotion of protocell self-assembly from mixed amphiphiles at the origin of life. *Nature ecology & evolution* **2019**, *3*, 1705−1714.
(49) Sarkar, S.; Das, S.; Dagar, S.; Joshi, M. P.; Mungi, C. V.; Sawant, A. A.; Patki, G. M.; Rajamani, S. Prebiological Membranes and Their Role in the Emergence of Early Cellular Life. *J. Membr. Biol.* **2020**, *253*, 589−608.
(50) Walde, P.; Ichikawa, S. Enzymes inside lipid vesicles: preparation, reactivity and applications. *Biomolecular engineering* **2001**, *18*, 143−177.
(51) Matsushita-Ishiodori, Y.; Hanczyc, M. M.; Wang, A.; Szostak, J. W.; Yomo, T. Using Imaging Flow Cytometry to Quantify and Optimize Giant Vesicle Production by Water-in-oil Emulsion Transfer Methods. *Langmuir* **2019**, *35*, 2375−2382.
(52) Morigaki, K.; Walde, P. Giant vesicle formation from oleic acid/sodium oleate on glass surfaces induced by adsorbed hydrocarbon molecules. *Langmuir* **2002**, *18*, 10509−10511.
(53) Schindelin, J.; Arganda-Carreras, I.; Frise, E.; Kaynig, V.; Longair, M.; Pietzsch, T.; Preibisch, S.; Rueden, C.; Saalfeld, S.; Schmid, B.; et al. Fiji: an open-source platform for biological-image analysis. *Nat. Methods* **2012**, *9*, 676−682.

https://doi.org/10.1021/acscentsci.1c01365
ACS Cent. Sci. 2022, 8, 132−139